Ab Initio Study of the Relative Basicity of the External Oxygen Sites in $M_2W_4O_{19}^{4-}$ (M = Nb and V)

Juan Miguel Maestre,[†] Jose Pedro Sarasa,[‡] Carles Bo,[†] and Josep M. Poblet*,[†]

Departament de Química Física i Inorgànica, Universitat Rovira i Virgili, Pc. Imperial Tarraco 1, 43005-Tarragona, Spain, and Departamento de Química Física y Química Orgánica, Universidad de Zaragoza, Ciudad Universitaria s/n, 50009-Zaragoza, Spain

Received February 29, 1996

Geometry optimizations were carried out for the cis and trans forms of $Nb_2W_4O_{19}^{4-}$. The energy difference between the two conformations was found to be 2.3 kcal mol^{-1}, the structure in which the two Nb atoms are in the cis formation being the most stable. Several isomers of the $Nb_2W_4O_{19}H^{3-}$ anion were also studied for the cis form, suggesting that the oxygen bonded to two Nb atoms is the most basic center. The energetic determination of the oxygen basicities in hexametalates was compared with the indirect and less computationally demanding methodology based upon molecular electrostatic potential (ESP) distributions. The ESP distribution in $HNb_2W_4O_{19}^{3-}$ suggests that a second proton should fix onto an OW_2 oxygen site and that the ONb terminal O's remain the most basic terminal centers. In $V_2W_4O_{19}^{4-}$, the unique OV_2 was identified as the most basic center. Although at variance with the niobotungstate anion, the most basic center does not support the highest net negative charge. The terminal OV oxygen sites were found to be the least basic terminal O's.

Introduction

Most of the current interest in polyoxometalates derives from the fact that they are relevant to catalysis, analytical chemistry, biology, medicine, and material science.[1−4] Their properties are related to their high charges and the strong basicity of the oxygen surfaces. Four isopolyanions are known to have a hexametalate structure, M_6O_{19}: $Nb_6O_{19}^{8-}$,[5] $Ta_6O_{19}^{8-}$,[6] $Mo_6O_{19}^{2-}$,[7] and $W_6O_{19}^{2-}$.[8] All of these anions present a structure close to O_h symmetry except for Mo_6O_{19} in $[HN_3P_3(NMe_2)_6]_2Mo_6O_{19}$, in which the distortion is considerable.[7a] Allcock et al. attributed this distortion to hydrogen bonds of the N−H···O type with the counterions.[7a] A more recent characterization by Clegg et al. reports a H-bond-free, practically undistorted anion structure.[7b] A series of niobotungstates $Nb_xW_{6-x}O_{19}^{(2+x)-}$ has also been isolated from aqueous solution.[9] Klemperer's group has recently reported several studies on the reactivity of $Nb_2W_4O_{19}^{4-}$,[10−13] **1**, and concluded that the ONb_2 oxygen is probably the most basic, nucleophilic oxygen site[10] (see Figure 1 for a diagram of **1**). From ^{17}O NMR experiments,[14] the unique OV_2 oxygen has been identified as the protonation site in the isoelectronic tungstovanadate $V_2W_4O_{19}^{4-}$ anion, **2**.

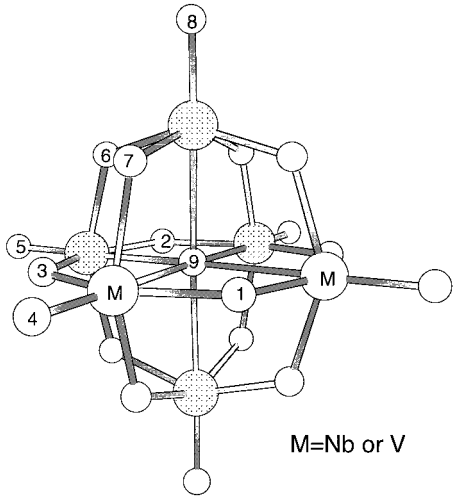

Figure 1. Structure of $M_2W_4O_{19}^{4-}$ (M = Nb or V).

In a previous paper, the relative basicity of the six distinct external oxygen sites of the decavanadate ion $V_{10}O_{28}^{6-}$ was studied by analyzing the topology of electrostatic potentials (ESP) and determining the charge concentrations near the oxygen sites. These distributions had been obtained from an

* Corresponding author.
† Universitat Rovira i Virgili.
‡ Universidad de Zaragoza.

(1) (a) Pope, M. T. *Heteropoly and Isopoly Oxometalates*; Springer-Verlag: New York, 1983. (b) Pope, M. T. In *Progress in Inorganic Chemistry*; Lippard, S. J., Ed.; Wiley: New York, 1991; Vol. 39, p 181. (c) Pope, M. T.; Muller, A. *Angew. Chem., Int. Ed. Engl.* **1991**, *30*, 34.
(2) Baker, L. C. W. In *Advances in the Chemistry of the Coordination Compounds*; Kirschner, S., Ed.; Macmillan: New York, 1961, p 608.
(3) Casañ-Pastor, N.; Baker, L. C. W. *J. Am. Chem. Soc.* **1992**, *114*, 10384.
(4) *Polyoxometalates: from Platonic Solids to Anti-Retroviral Activity*, Pope, M. T.; Muller, A., Eds.; Kluwer Academic Publishers: Dordrecht, The Netherlands, 1994.
(5) Lindqvist, I. *Ark. Kemi* **1952**, *5*, 247.
(6) Lindqvist, I.; Aronsson, B. *Ark. Kemi* **1954**, *7*, 49.
(7) (a) Allcock, H. R.; Bisell, E. C.; Shawl, E. T. *Inorg. Chem.* **1973**, *12*, 2963. (b) Clegg, W.; Sheldrick, G. M.; Garner, C. D.; Walton, I. B. *Acta Crystallogr.* **1982**, *B38*, 2906.
(8) Fuchs, J.; Freiwald, W.; Hartl, H. *Acta Crystallogr.* **1978**, *B34*, 1764. Ming-Quin, C.; Si−San, Z.; Yi-Dong, G. *J. Struct. Chem.* **1990**, *9*, 26.
(9) Dabbabi, M.; Boyer, M. J. *Inorg. Nucl. Chem.* **1976**, *38*, 1011.
(10) Day, V. W.; Klemperer, W. G.; Schwartz, C. *J. Am. Chem. Soc.* **1987**, *109*, 6030.
(11) Besecker, C. J.; Day, V. W.; Klemperer, W. G.; Thompson, M. R. *J. Am. Chem. Soc.* **1984**, *106*, 4125.
(12) Day, V. W.; Klemperer, W. G.; Main, D. J. *Inorg. Chem.* **1990**, *29*, 2345. Klemperer, W. G.; Main, D. J. *Inorg. Chem.* **1990**, *29*, 2355.
(13) Beseker, C. J.; Klemperer, W. G. *J. Am. Chem. Soc.* **1980**, *102*, 7598.
(14) Klemperer, W. G.; Shum, W. *J. Am. Chem. Soc.* **1978**, *100*, 4891.

S0020-1669(96)00222-4 CCC: $15.00
Published on Web 05/20/1998

Table 1. Bond Lengths for $W_6O_{19}^{2-}$ Anion[a]

	W−O_t	W−O_b	W−O_c
computed	1.708	1.926	2.403
X-ray[b]	1.69	1.92	2.33

[a] Values are in Å. O_t, terminal oxygens; O_b, bridging OM_2 oxygens; O_c, central, OM_6 oxygen. [b] Values averaged to O_h symmetry, ref 8.

ab initio SCF wave function.[15] The investigations on the decavanadate anion showed that the basicity of the oxygen atoms in polyoxometalates is directly related to the oxygen type. The relative oxygen basicity order was found to be OV_3 (triple-bridging) oxygen > OV_2 (double-bridging) oxygen > OV (terminal) oxygen. However, the basicity difference between two oxygen atoms connected to the same number of metal centers is quite small, and therefore, their classification is more difficult. The main goal of the present study is to directly determine a basicity scale for double-bridging oxygens in $M_2W_4O_{19}^{4-}$ for M = Nb (**1**) and V(**2**) by calculating the relative energy of the corresponding protonated anion. The relatively small M_6O_{19} framework allows the geometries for $M_2W_4O_{19}^{4-}$ and $M_2W_4O_{19}H^{3-}$ to be computed. The electrostatic potentials and the Laplacian of the charge density distributions are also derived for anions **1** and **2** and analyzed in connection with the relative energies of the protonated anions.

Computational Details

The geometries and energies were determined at the Hartree−Fock level, using the TURBOMOLE program.[16] Since the metal atoms are formally d^0, correlation effects are not of the utmost importance, and the HF approach should be appropriate. The basis sets used for geometry optimizations (basis set I) are defined as follows: V, Nb, and W, a Hay and Wadt effective core potential[17] models the potential of the inner electrons. The 13 valence electrons of V and Nb are described by a (8s, 5p, 5d) and (8s, 6p, 4d) basis set, respectively, contracted into [3s/3p/2d]. The 14 valence electrons of W are described by a (8s, 6p, 3d) basis set also contracted into [3s/3p/2d].[17]

O and H: Double-ζ Bases by Huzinaga.[18] Single point calculations were carried out using basis set II in which the valence shell of the oxygen atoms, formally O^{2-}, are represented with an extended basis set composed of 6s-type and 4p-type contracted Gaussians, and two polarization functions.[19]

Electrostatic potentials were computed for planar grids of points defined in planes containing several oxygen sites. Minima in the ESP distribution were located by gradient procedures. The topological properties of the charge density were determined using the AIMPAC package of programs.[20] Finally, the integrations of the charge density were carried out with ATOMICI-VECSURF,[21] a modified version of the original PROAIM program.[20]

To check if the geometries were well reproduced at the proposed level, we optimized the $W_6O_{19}^{2-}$ anion structure in O_h symmetry with basis set I. From the bond distances given in Table 1, we can see that W−O_t (O_t: terminal oxygen) and W−O_b (O_b: bridging oxygen) computed bond distances are in good agreement with the X-ray parameters. The discrepancies are less than 0.02 Å. For the weaker interaction between the tungsten atoms and the central oxygen, the calculated distance is 2.403 Å, 0.07 Å longer than the averaged W−O_c distances (O_c: central oxygen). An interpretation of the structure of the inclusion complexes R−CN ⊂ $(V_{12}O_{32})^{4-}$ from electrostatic potentials has also been carried out at the HF level by Benard and co-workers.[22]

Polyoxometalate anions most often are highly charged species, which are only observed in solution or in solid phase. The presence of counterions in the vicinity of the anion raises the potential and stabilizes the cluster. Recently, a procedure has been developed by Benard and co-workers in order to model the crystal field in studies of polyoxometalates.[23] The procedure reproduces the electrostatic potential generated by the crystal by means of an isotropic field created by a charged sphere located at a large distance from the cluster. That model was used in the study of the interaction energy between the anionic host $(HV_{18}O_{42})^{8-}$ and the Cl^- guest anion and in the analysis of the redox properties of the highly reduced Keggin anion $PMo_{12}O_{40}(VO)_2^{5-}$.[23] In both cases, the calculations showed that the inclusion of the crystal field dramatically decreases the energy of the frontier orbitals but does not alter the electronic structure of the free anion. Such a procedure, however, requires a good X-ray description of the crystal structure including an unambiguous characterization of the counterions. This prerequisite was not fulfilled in the present case because of disorder problems in the crystal structure. The authors think, however, that the inclusion of the counterion effects would not modify the main conclusions in the present work since they rely on the relative properties of the distinct oxygen sites in an anion.

Results and Discussion

Structure of $Nb_2W_4O_{19}^{4-}$. The optimal structures and their relative energies for cis and trans configurations of $Nb_2W_4O_{19}^{4-}$ were computed. The optimized trans structure with D_{4h} symmetry was found to be 1 kcal mol^{-1} less stable than the cis isomer with C_{2v} symmetry. Single point calculations carried out with basis set II increased the energy gap in favor of the cis form to 2.3 kcal mol^{-1}. The main difference between the D_{4h} and C_{2v} structures is the presence of a permanent dipole moment in the isomer where the Nb atoms are cis. These relative energetic values are in agreement with IR and RAMAN studies, which suggest that the symmetry of $Nb_2W_4O_{19}^{4-}$ is C_{2v}.[24] The C_{2v} geometry was also found to be the most stable form for the isoelectronic tungstovanadate anion **2**. The energy difference between the cis and trans forms is 3 kcal mol^{-1} with basis set I.[25] Bond distances for **1** are collected in Table 2. No direct structural information is available for mixed isopolyanions such as **1** since X-ray characterization of these kinds of compounds is plagued with disorder problems.[10−13] However, good approximations to the Nb−O bond lengths may be found from the related structures of $Mn(Nb_6O_{19})_2^{12-}$ or $Nb_{10}O_{28}^{6-}$. The expected distances should be Nb−O (terminal) ∼1.73−1.76, Nb−O (bridging) ∼1.95−2.10, and Nb−O (central) ∼2.4 Å.[26] From the values in Table 2 we can see that the computed Nb−O bond lengths are in the right range and that they do not differ significantly from the W−O bond distances.

Electrostatic Potential Distributions and Relative Protonation Energies. In Figure 2 the ESP distribution is displayed in the plane containing oxygens 1−5. Constant contour intervals (0.011 au) were selected for the plane diagram, the lowest value

(15) Kempf, J. Y.; Rohmer, M.-M.; Poblet, J. M.; Bo, C.; Bénard, M. *J. Am. Chem. Soc.* **1992**, *114*, 1136.
(16) TURBOMOLE: a direct SCF program from the Quantum Chemistry Group of the University at Karlsruhe under the directorship of Prof. R. Ahlrichs, *Chem. Phys. Lett.* **1989**, *162*, 165.
(17) Hay, P. J.; Wadt, W. R. *J. Chem. Phys.* **1985**, *82*, 270.
(18) Huzinaga, S. *Approximate Atomic Functions, Technical Report*, University of Alberta: Canada, 1971.
(19) Hyla-Kryspin, I.; Demuynck, J.; Strich, A.; Benard, M. *J. Chem. Phys.* **1981**, *75*, 3954.
(20) Biegler-Konig, F. W.; Bader, R. F. W.; Tang, T. H. *J. Comput. Chem.* **1982**, *3*, 317.
(21) Cioslowski, J.; Nanayakara, A.; Challacombe, M. *Chem. Phys. Lett.* **1993**, *203*, 137. Cioslowski, J. *J. Chem. Phys.* **1992**, *194*, 73.
(22) Rohmer, M.-M.; Benard, M. *J. Am. Chem. Soc.* **1994**, *116*, 6959.
(23) Blaudeau, J. P.; Rohmer, M.-M.; Rohmer, Benard, M.; Ghermani, N. E. *Bull. Chim. Soc. Fr.*, in press. Rohmer, M. M.; Bénard, M.; Blaudeau, J. P.; Maestre, J. M.; Poblet, J. M., submitted for publication. Maestre, J. M.; Bo, C.; Poblet, J. M.; Casañ-Pastor, N.; Gomez-Romero, P., submitted for publication.
(24) Rocchiccioli-Deltcheff, C.; Thouvenot, R.; Dabbabi, M. *Spectrochim. Acta* **1977**, *33A*, 143.
(25) Using all electron basis sets, we found the energy gap between D_{4h} and C_{2v} isomers for $V_2Mo_4O_{19}^{4-}$ to be 1 kcal mol^{-1}.
(26) Reference 1a, pp 40−41.

Table 2. Bond Distances (in Å) Computed for $Nb_2W_4O_{19}^{4-}$ **1** and $V_2W_4O_{19}^{4-}$ **2**[a,b]

M−O_t		M−O_b		M−O_c	
		$Nb_2W_4O_{19}^{4-}$			
Nb−O_4	1.761	Nb−O_1	1.959	Nb−O_9	2.503
W_1−O_5	1.729	Nb−O_3	2.048	W_1−O_9	2.322
W_2−O_8	1.727	Nb−O_7	2.027	W_2−O_9	2.374
		W_1−O_2	1.937		
		W_1−O_3	1.866		
		W_1−O_6	1.920		
		W_2−O_6	1.949		
		W_2−O_7	1.873		
		$V_2W_4O_{19}^{4-}$			
V−O_4	1.566	V−O_1	1.801	V−O_9	2.428
W_1−O_5	1.735	V−O_3	1.918	W_1−O_9	2.232
W_2−O_8	1.732	V−O_7	1.868	W_2−O_9	2.331
		W_1−O_2	1.952		
		W_1−O_3	1.862		
		W_1−O_6	1.929		
		W_2−O_6	1.947		
		W_2−O_7	1.872		

[a] O_t, terminal oxygens; O_b, bridging OM_2 oxygens; O_c, central, OM_6 oxygen. [b] See Figure 1 for numeration.

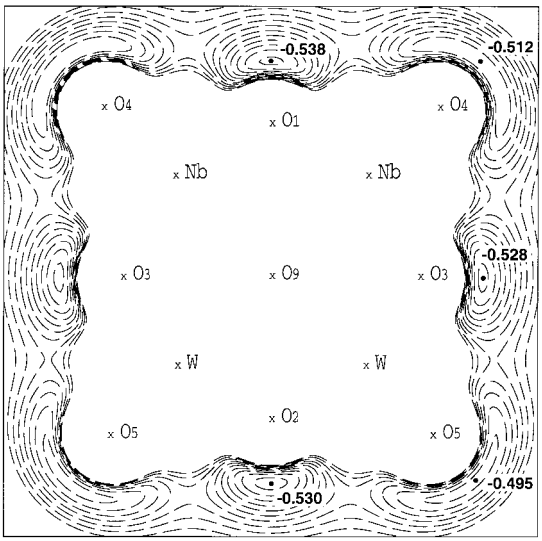

Figure 2. Section of the electrostatic potential (ESP) for $Nb_2W_4O_{19}^{4-}$: Nb_2W_2 plane containing one O_1, one O_2, two O_3, two O_4, and two O_5 oxygen sites; highest contour, −0.424 au; lowest contour, −0.538 au; contour interval, −0.011 au. The black dots denote the positions of the distinct ESP minima in this plane. The deepest minimum is located in the vicinity of the ONb_2 oxygen.

starting at −0.538 au. In the vicinity of each oxygen site, a minimum in the ESP distribution was detected. The deepest minimum appears facing O_1, the unique ONb_2 oxygen. The minima associated with O_2 (an OW_2 oxygen site) and O_3 (an ONbW oxygen site) are only 5.3 and 6.4 kcal mol^{-1} higher, respectively, than that of the potential well connected with O_1. The minima associated with the terminal oxygen sites 4 and 5 are higher than that of O_1 by 16 and 27 kcal mol^{-1}, respectively. This behavior is widespread in polyoxoanions; minima connected with terminal oxygens are markedly higher than those associated with bridging oxygens. This tendency is also followed by the potential wells detected near O_6, O_7, and O_8. All the ESP minima found for the distinct oxygen sites are summarized in Table 3.

Using basis set I, we analyzed six $HNb_2W_4O_{19}^{3-}$ isomers, **3**, corresponding to the protonation sites of the distinct external oxygen atoms on the Nb_2W_2 plane and the protonation at O_8. One of the constraints was that all geometries computed for **3** had to retain a symmetry plane; therefore, for the additions at the O_3, O_4, and O_5 oxygen sites, the hydrogen atom was not allowed to bend out of the Nb_2W_2 plane. The two other possible conformations without symmetry elements were not calculated since the study of structures with C_1 symmetry (protonations at O_6 and O_7) demands an enormous computational effort. Moreover, it can be estimated that the basicities of O_6 and O_7 must be only marginally different from those of O_2 and O_3, respectively.

Table 3. Atomic Net Charges (Q), Relative Values of ESP Minima (in kcal mol^{-1}), and Relative Protonation Energies (E_r, in kcal mol^{-1}) computed for $Nb_2W_4O_{19}^{4-}$ **1** Using Basis Set I and II

		Q[b]		ESP		
atom[a]	type	I	II	I	II	E_r[e]
O_1	ONb_2	−1.33	−1.39	0.0[c]	0.0[d]	0.0
O_2	OW_2	−1.31	−1.38	5.3	2.4	3.1
O_3	ONbW	−1.30	−1.37	6.4	3.4	3.8
O_4	ONb	−1.17	−1.31	16.5	11.6	8.9
O_5	OW	−1.12	−1.26	27.3	24.8	25.4
O_6	OW_2	−1.31	−1.37	7.6	2.6	
O_7	ONbW	−1.31	−1.37	7.7	3.2	
O_8	OW	−1.11	−1.26	28.5	26.6	24.7
O_9	OM_6	−1.59	−1.55			
metal						
Nb_1		+3.12	+3.32			
W_1		+3.46	+3.76			
W_2		+3.46	+3.76			

[a] See Figure 1 for oxygen atom numeration. [b] Determined from density integration of the atomic basin (Bader's method). [c] The absolute value is −0.5381 au. [d] The absolute value is −0.5144 au. [e] Basis set I.

According to the experimental evidence the proton fixation occurs predominantly at the unique bridging ONb_2 oxygen. Consequently, the structure in which the hydrogen atom is bonded to O_1 is found to be the most stable isomer. This conformation was optimized with a C_s symmetry but also under the constraints of the C_{2v} point group. The relative energy of the C_s geometry with respect to the relative energy of the C_{2v} form is close to 0.5 kcal mol^{-1}, which means that the hydrogen-bending energy is almost negligible. Some bond distances for **3** are given in Figure 3. The values in parentheses in Figure 3 represent the changes in the bond separation from the unprotonated precursor. The formation of the H−O bond leads to a considerable lengthening of the bond between the niobium atoms and the protonated oxygen (0.187 Å). The weakening of these bonds increases the interaction between the Nb atoms and all other bonded oxygens, shortening the bonding distances. Even though some W−O bond lengths in the Nb_2W_2 plane are altered by protonation, the overall distortion in the rest of the molecule is noticeably lower.

The relative energies of the H−O_2 and H−O_3 isomers (the hydrogen is bonded to O_2 and O_3, respectively) were computed to be 3.1 and 3.8 kcal mol^{-1}, respectively. In these two isomers the conformation lowest in energy has the hydrogen atom out of the Nb_2W_2 symmetry plane. The structures corresponding to the protonation of the terminal oxygen atoms 4 and 5 were also optimized. Their relative energies with respect to the most stable conformation (H−O_1) were computed to be 8.9 and 25.4 kcal mol^{-1}, respectively. Thus, the calculated relative energies, which are given in Table 3, fully confirm the estimations made by Klemperer,[10] who proposed that the bridging oxygens are more basic than the terminal oxygens, the ONb_2 site being the most basic center. Moreover, our relative energetic data strongly suggest that in $Nb_2W_4O_{19}^{4-}$, the ONb oxygens have basicities significantly greater than those of the terminal OW oxygens.

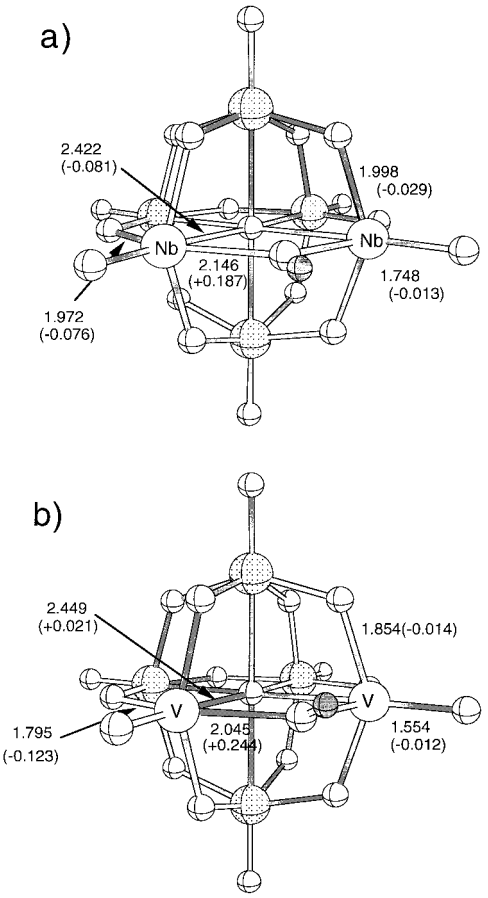

Figure 3. Optimized geometry for the most stable conformation of $HNb_2W_4O_{19}^{3-}$ (a) and $HV_2W_4O_{19}^{3-}$ (b). Selected bond distances are in Å. Major bond changes with respect to the unprotonated anions **1** and **2** are given in parentheses.

All the Cartesian coordinates computed for the six isomers of anion **3** are given as Supporting Information.

Let us now analyze the relative energies of the protonated ions in connection with the depth of the potential well facing the protonated oxygen site and with the atomic charge density of the protonated oxygen. The atomic population analysis proposed by Bader et al.[27] consists of defining the atomic domain as the three-dimensional basin limited by the surfaces of zero gradient-flux.[33] Using basis set I, we carried out charge integration on such domains for all atoms of anion **1**. The net charge obtained is −1.59 e for the oxygen atom located inside the cage and connected to six metal atoms. The hexametalate clusters $M_6O_{19}^{n-}$ have been described as an $M_6O_{18}^{(n-2)-}$ framework with an O^{2-} species inside the cage.[28] The high electronic population of O_9 indicates that this description is quite appropriate. All the bridging oxygens exhibit considerable net charges (Table 3), the largest value being computed for the unique ONb_2 oxygen atom (−1.33 e). This behavior was also found for terminal oxygen sites. An ONb oxygen supports an electron population density higher than that for a terminal oxygen connected to a tungsten atom. This can be interpreted from the relative orbital energies of Nb and W atoms.[17] The niobium atoms can transfer more charge density to the oxygen sites since their atomic orbitals are higher in energy than those of tungsten atoms. As a matter of fact, the Bader population analysis assigns net charges of +3.12 and +3.46 e to Nb and W atoms, respectively. This means that, whereas niobioum atoms transferred 62% of their valence electrons to oxygens, tungsten atoms transferred 57%. These charge-transfer values confirm the high ionic character of the metal−oxygen interaction in cluster **1**. Actually, the depth of the potential well facing an oxygen site increases with the negative net charge of the oxygen core (Table 3). Therefore, the *relative protonation energy of an oxygen site appears to be strongly correlated to the corresponding ESP minimum and to the Bader charge of the protonated oxygen atom*. This relationship indicates that the proton fixation in $Nb_2W_4O_{19}^{4-}$ is mainly driven by electrostatic forces.

The use of basis set II slightly increases the charge transfer from the metal atoms to the oxygen cores but does not modify the basicity scale of the distinct oxygen sites in anion **1**. The inclusion of diffuse orbitals and polarization functions in all oxygen centers, however, diminishes the basicity difference of the oxygens. With basis set II, the electron population difference between the most and least populated external oxygen atoms (O_1 and O_5, respectively) is −0.13 e, whereas the corresponding value with basis set I is −0.21 e. The effect of polarization functions appears to be quite important in the ESP distribution around the oxygen sites. With the smaller basis set, the ESP distribution exhibits a minimum per oxygen. All these ESP minima become saddle points which connect two new minima when the extended basis set II is used. The ESP minima associated with O_1, O_2, and O_3 are now placed above and below the Nb_2W_2 symmetry plane. The ones associated with oxygens 6 and 7 are also out of the *pseudo*-NbW_3 planes. Drawing **5** displays the XOX angles (X = ESP_{min}) and the relative energy values of the ESP saddle points with respect to the ESP local minima for the most basic oxygens (O_1 and O_2).

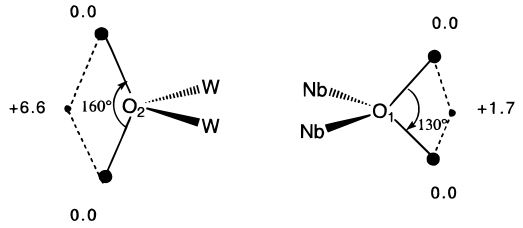

5

In the case of the ONb_2 oxygen, the XOX angle is 130°, and the energy difference between the minima and the saddle point is only 1.7 kcal mol^{-1}. These values suggest that if the reoptimization of the most stable isomer of $HNb_2W_4O_{19}^{3-}$ (the hydrogen atom is bonded to O_1) with basis set II were carried out, the most stable conformation for this isomer should belong to the C_s symmetry point group rather than to the C_{2v} minimum found with basis set I. Presently, this kind of calculation is still formidable and has not been carried out. In any case, we think that the energy difference between the C_s and C_{2v} conformations would not be very high. The values of the ESP stationary points found near O_2 (**5**) indicate that this oxygen presents a less spherical distribution of its charge density, the relative energy of the saddle point with respect to the local minima being +6.6 kcal mol^{-1}. Therefore, any protonation of this oxygen should take place out of the Nb_2W_2 plane. At variance with the minima corresponding to bridging oxygens, the two ESP minima connected with O_4 and O_5 remain on the Nb_2W_2 plane when calculations are carried out with basis set II. The minima associated with O_8 are located on the symmetry plane that contains this terminal oxygen. The energy difference between the ESP saddle point and the corresponding minima is about 5 kcal mol^{-1} for all terminal oxygens.

(27) Bader, R. F. W. *Atoms in Molecules. A Quantum Theory*; Clarendon Press: Oxford, 1990; Bader, R. F. W. *Chem. Rev.* **1992**, *91*, 893.
(28) Anne Dolbecq, Ph. D., Paris XI, Orsay, 1995.

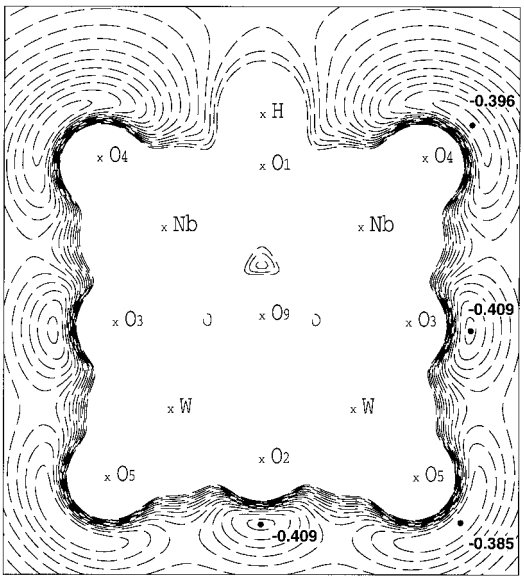

Figure 4. Section of the electrostatic potential (ESP) for $HNb_2W_4O_{19}^{3-}$: Nb_2W_2 plane containing one O_1, one O_2, two O_3, two O_4, and two O_5 oxygen sites; highest contour, −0.182 au; lowest contour, −0.405 au; contour interval, −0.016 au. The black dots denote the positions of the distinct ESP minima in this plane.

ESP Distribution in $HNb_2W_4O_{19}^{3-}$. The distribution of the electrostatic potential on the plane containing the hydrogen atom and sites O_1 and O_5 is shown in Figure 4. The comparison between Figures 2 and 4 shows that the proton fixation modifies the ESP distribution near the protonated oxygen site quite considerably, but modifies the ESP distribution very little in the proximity of the other oxygens. The absolute values, however, are lower than those of the unprotonated partner since the depth of the potential wells correlates with the anion charge. In less charged anions, the protonation effect is quite different. For instance, in the case of the divalent $Mo_6O_{19}^{2-}$, the fixation of a proton induces an important modification of the ESP distribution of the terminal and bridged oxygen sites nearest the bridged protonated oxygen.[29] In the niobotungstate anion, upon protonation, the minima associated with the unprotonated bridging oxygen sites exhibit similar depth, the energy difference being lower than 0.2 kcal mol^{-1}. Another interesting feature of Figure 4 is the presence of a quite deep minimum close to the oxygen site which is nearest to the protonated center. According to the ESP distribution, the terminal ONb site is still the most basic terminal oxygen after protonation. This minimum is less stable than the one associated with O_2 by 8.4 kcal mol^{-1} (Table 5).

The integrated net charges confirm that protonation induces a low electronic perturbation on the cluster. According to Bader's method, the population of the hydrogen atom is as high as 0.42 e. The corresponding depopulation of the M_6O_{19} framework mainly occurs in terminal O's, each terminal oxygen core losing approximately 0.05 e. The charges in Tables 3 and 5 show that the proton fixation does not modify the electron population of the protonated center.

The Tungstovanadate Anion $V_2W_4O_{19}^{4-}$. From NMR studies, Klemperer and Shum[14] have identified the unique OV_2 oxygen in $V_2W_4O_{19}^{4-}$, an isoelectronic anion of the niobotungstate anion **1**, as the protonation site. We carried out HF calculations and geometry optimizations on $V_2W_4O_{19}^{4-}$, **2**, and on five isomers of the protonated ion using basis set I. Selected bond distances for anion **2** are given in Table 2. The reader can see from bond distances of Table 2 that the structure of anion **2** is very similar to that of anion **1**. The only noticeable differences are related to the substituted fragment because of the different nature of the metal center.

(29) Benard, M.; Rohmer, M.-M., unpublished work.

Table 4. Atomic Net Charges (*Q*), Relative Values of ESP Minima (in kcal mol^{-1}), and Relative Protonation Energies (E_r, in kcal mol^{-1}) Computed for $V_2W_4O_{19}^{4-}$ **2** Using Basis Set I and II

		Q^b		ESP		
atom[a]	type	I	II	I	II	E_r[e]
O_1	OV_2	−1.16	−1.22	0.0[c]	0.0[d]	0.0
O_2	OW_2	−1.31	−1.38	-4.1	2.8	5.2
O_3	OVW	−1.24	−1.31	-0.8	1.4	5.1
O_4	OV	−0.89	−1.03	36.8	33.4	38.7
O_5	OW	−1.13	−1.28	19.4	27.7	30.1

[a] See Figure 1 for oxygen atom numeration. [b] Determined from density integration of the atomic basin (Bader's method). [c] The absolute value is −0.5397 au. [d] The absolute value is −0.5829 au. [e] Basis set I.

Table 5. Atomic Net Charges (*Q*), Relative Values of ESP Minima (in kcal mol^{-1}) and Computed for $HNb_2W_4O_{19}^{3-}$ **3** and $HV_2W_4O_{19}^{3-}$ **4** Using Basis Set I

atom	type	Q (M = Nb)	ESP (M = V)	Q (M = Nb)	ESP (M = V)
O_1	OM_2	1.33		−1.24	−4.15
O_2	OW_2	−1.29	0.0[a]	−1.29	0.0[b]
O_3	OMW	−1.30	0.2	−1.22	3.1
O_4	OM	−1.12	8.4	−0.84	36.6
O_5	OW	−1.05	15.1	−1.06	15.5
hydrogen[c]		+0.58		+0.55	

[a] The absolute value is −0.4093 au. [b] The absolute value is −0.4185 au. [c] The hydrogen atom is bonded to O_1.

The atomic charge density was computed for several external oxygen sites of anion **2**. In contrast to anion **1**, an elementary examination of the oxygen net charges is not enough to predict the most basic oxygen site in $V_2W_4O_{19}^{4-}$ (see Table 4). For example, the integration method assigns a net charge of −1.16 e to the bridging OV_2 oxygen, whereas the corresponding value for O_2, a bridging OW_2 oxygen, is −1.31 e. The net charges obtained for the terminal oxygens O_4 and O_5 are −0.89 e and −1.13 e, respectively. Thus, oxygens bonded to vanadium atoms support an electronic charge density lower than that for oxygens connected to tungsten atoms. The oxygen charge density in polyoxoanions depends heavily on the oxygen type and, to a lesser extent, on the specific molecule. The O_2 and O_5 net charges for instance, are identical in anions **1** and **2**. Another interesting example is that of the terminal OV oxygen sites. The computed value for O_4 in $V_2W_4O_{19}^{4-}$ (−0.89 e) is similar to the values reported for the decavanadate anion,[15] in which net charges of −0.85 e and −0.89 e were found for the two distinct terminal oxygen sites, respectively. As in the niobotungsten anion, the inclusion of diffuse functions and d polarization orbitals in all oxygen atoms increases somewhat the charge transfer from metals to oxygens, the highest increment taking place in the terminal oxygens.

The next section will be devoted to the analysis of the ESP distribution around the external oxygen sites located on the V_2W_2 plane. The number and space distribution of the potential minima computed using basis set I is not significantly different from those obtained for anion **1**. Figure 5 displays the section of the electrostatic potential for $V_2W_4O_{19}^{4-}$ containing sites 1−5. According to the atomic charges, the deepest minimum of the ESP distribution is found in the vicinity of the O_2 site. The minima associated with the bridging OV_2 oxygen site is 4.1

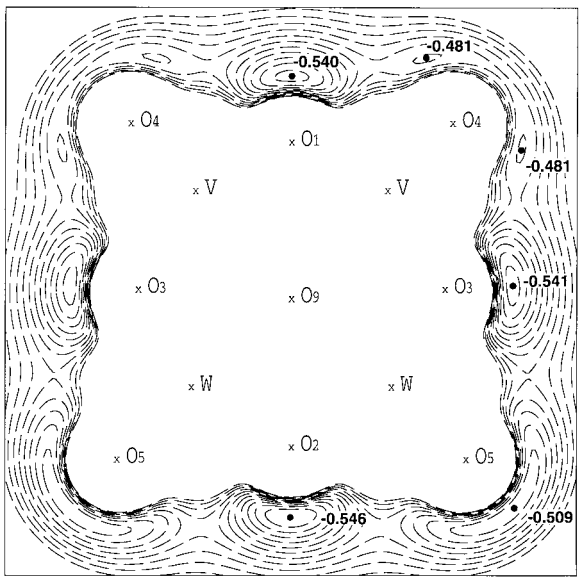

Figure 5. Section of the electrostatic potential (ESP) for $V_2W_4O_{19}^{4-}$: V_2W_4 plane containing one O_1, one O_2, two O_3, two O_4, and two O_5 oxygen sites; highest contour, −0.424 au; lowest contour, −0.583 au; contour interval, −0.011 au. The black dots denote the positions of the distinct ESP minima. The deepest minimum with basis set I is located near the OW_2 oxygen. With the largest basis set II, the ESP minimum near the OV_2 oxygen is the deepest (see text).

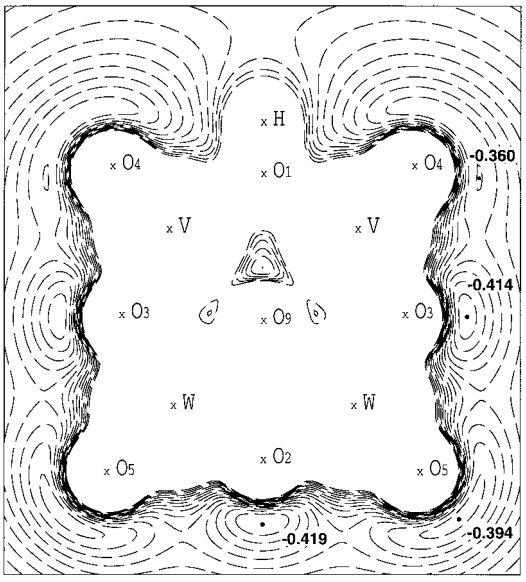

Figure 6. Section of the electrostatic potential (ESP) for $HV_2W_4O_{19}^{3-}$: V_2W_4 plane containing one O_1, one O_2, two O_3, two O_4, and two O_5 oxygen sites; highest contour, −0.182 au; lowest contour, −0.405 au; contour interval, −0.016 au. Dots indicate the positions of the distinct ESP minima.

kcal mol^{-1} higher than the potential well connected with O_2. The minimum found near the OVW site is also lower than that associated with O_1. The relative depth of minima connected to terminal and bridging oxygens reproduces the trend described for anion **1** (Table 3). The results on ESP distribution, however, do not rationalize the protonation site for $V_2W_4O_{19}^{4-}$ since O_1 has been identified as the most attractive site for protons.[14] In fact, the problem arises because of the inability of basis I to discern between similar oxygen sites. Again, the minima found near each bridging oxygen transforms into saddle points when basis set II is used. These points connect two minima placed above and below the V_2W_2 plane. With the extended basis set, the ESP distribution has its deepest minimum in the vicinity of the unique OV_2 oxygen site. This is in complete agreement with the protonation data. The potential well connected with an OV site is 6 kcal mol^{-1} higher than the well associated with an OW site. Thus, the ESP data suggest that the oxygen sites bonded to only one vanadium center are by far the least basic oxygen sites in anion **2**. This may be explained by the lower net charge supported by these single-bonded oxygens. The atomic net charges and the relative values of the ESP minima for $V_2W_4O_{19}^{4-}$ are summarized in Table 4.

The isomers corresponding to the O_1 and O_2 protonations were optimized with basis set I. The optimization process yielded the lowest energy for the conformation in which the hydrogen atom is bonded to the OV_2 oxygen site. The energy difference between the two isomers was found to be 5.2 kcal mol^{-1}. This shows that relative protonation energies can be computed with a relatively small basis set. At variance from anion **1**, protonation considerably modifies the ESP distribution in the protonated hemisphere. Figure 6 shows the contour map of electrostatic potential for the V_2W_2 plane. It can be seen that, near the OV oxygen, only the minimum closest to O_3 remains upon protonation, its energy being 37 kcal mol^{-1} with respect to the energy of the minimum connected with O_2, the deepest potential well on the V_2W_2 plane. The second deepest minimum is facing the OVW oxygen site. Its relative energy, with respect to the minimum near O_2, is not modified by protonation (∼3 kcal mol^{-1}). The relative depth between the stationary points associated with the OV and the OW O's increases by 4 kcal mol^{-1} due to proton fixation. According to the present calculations, OV oxygen sites remain the least basic terminal centers of the polyoxoanion. The most interesting result for the $HV_2W_4O_{19}^{3-}$ anion (**4**) is, however, the presence of a minimum connected to the protonated OV_2 oxygen site which is 4.1 kcal mol^{-1} lower than the minimum found near O_2. Anion **4** was optimized in C_{2v} and C_s symmetries, **6**. In contrast to anion $HNb_2W_4O_{19}^{3-}$, the geometry with symmetry C_{2v} is computed to be higher in energy than the geometry in which the hydrogen atom is allowed to bend out of the V_2W_2 plane, **6**. As a matter of fact, the minimum in the ESP distribution found in the vicinity of protonated site O_1 appears in the nonbonding region opposite the tripod formed by one hydrogen atom and two vanadium atoms. The comparison of the atomic net charges computed for anion **4** (Table 5) and the charges of its precursor (Table 4) leads us to conclude that proton fixation *increases* the atomic charge density of the protonated oxygen. The net charge of the hydrogen atom is +0.55 e; therefore oxygen O_1 is connected to three positively charged atoms. This could explain the most basic character predicted for O_1 from the ESP distribution since oxygen O_1 in **4** has a certain triple bridging nature. It should be pointed out that ESP studies on $HV_2W_4O_{19}^{3-}$ were only carried out with the smallest basis set and that the use of larger basis sets may slightly modify the present conclusions.

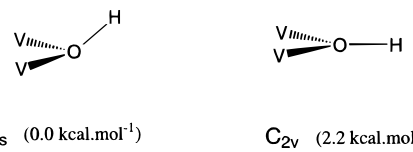

C_s (0.0 kcal.mol^{-1}) C_{2v} (2.2 kcal.mol^{-1}) **6**

The final section analyses the distribution of the Laplacian of charge density ($\nabla^2\rho$) around bridging oxygens O_1 and O_2 for anions **2** and **4**. The map of Figure 7 shows that the distibution of $\nabla^2\rho$ around the oxygen atoms exhibits a very low polarization. The Laplacian of charge density remains close to

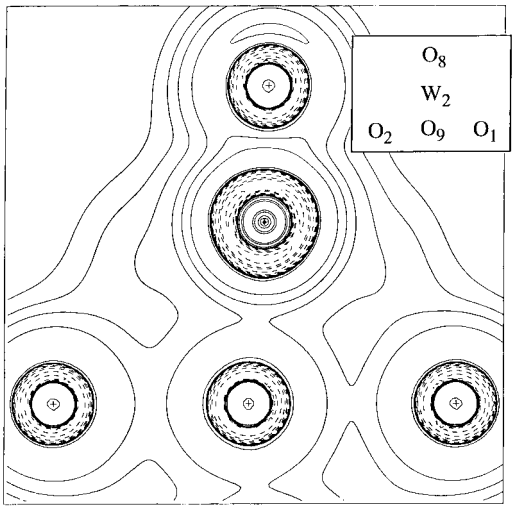

Figure 7. Laplacian of ρ plot for $V_2W_4O_{19}^{4-}$ in a plane containing oxygens O_1, O_2, O_8, and O_9. The solid contour lines correspond to positive values of $\nabla^2\rho$, the dashed ones to negative values. The contour values in au are ±0.002, ±0.004, and ±0.008, increasing in powers of 10 to ±8.0. The outermost contour is 0.002 au.

the spherical symmetry for all oxygen sites, which is consistent with their high negative charge. In ionic bonds,[30−32] the negatively charged atom exhibits small charge concentrations in the nonbonding region. In the case of oxygen O_2 which bridges between two W atoms, the laplacian of ρ presents two symmetric maxima in the nonbonding region above and below the V_2W_2 plane. These maxima of charge concentrations have a value of -5.09 au for $\nabla^2\rho$. In the nonbonding region of the OV_2 site, two maxima were also found. Despite the lower negative charge of O_1, the corresponding value for the Laplacian of ρ maxima is -5.15 au. This demonstrates the role of local factors in determining the position and magnitude of the ESP minima. Proton fixation of site O_1 only slightly modifies the valence shell of O_2, the two maxima increasing their value up to -5.15 au. However, the valence shell of the protonated oxygen has only one charge concentration in the nonbonding region. Probably related to the fact that the O_1 site is connected to three positively charged atoms, the corresponding $\nabla^2\rho$ value is -6.85 au, notably higher than the charge accumulations detected in the other double-bridged oxygens of the molecules studied. The deepest ESP minimum found in the vicinity of O_1 in anion **4** may be caused by the considerable charge concentration opposite the V_2H tripod.

Conclusions

In the present work we have reported the first ab initio calculations on hexametalate anions. These calculations have reproduced the geometries very well and determined the basicity of the external oxygens. Even though geometry optimizations of polyoxoanions at the ab inito−HF level still require considerable computational effort, ab initio calculations can help to characterize hexametalate structures since in these kinds of compounds, the X-ray determinations often present disorder problems.

In the $Nb_2W_4O_{19}^{4-}$ anion, the deepest minimum in the ESP distribution appears near the unique ONb_2 oxygen site. Accordingly, and in full agreement with experimental protonation data, the conformation of lowest energy for $HNb_2W_4O_{19}^{3-}$ corresponds to the structure in which the hydrogen atom is bonded to the ONb_2 oxygen, the most basic nature of which may be explained by the highest net charge supported by this oxygen. In the isoelectronic tungstovanadate anion, $V_2W_4O_{19}^{4-}$, the situation is slightly different. The relative protonation energies and the ESP distribution identify the least populated bridging OV_2 oxygen as the most basic center. The terminal OV O's are by far the least basic oxygen sites. The ESP distribution in $HNb_2W_4O_{19}^{3-}$ suggests that a second proton should fix onto an OW_2 oxygen site and that the ONb terminal O's are still the most basic terminal centers. ESP distribution for the $HV_2W_4O_{19}^{3-}$ anion suggests that the protonated OV_2 oxygen has a considerable basic nature.

Acknowledgment. HF calculations were carried out on workstations purchased with funds provided by the DGICYT of the Government of Spain and by the CIRIT of the Generalitat of Catalunya (Grants PB95-0639-C02-02 and SGR95-426). We thank Professor J. Cioslowski for a Cray version of the PROAIM program. The charge density was integrated on the CRAY-YMP of the Centre de Supercomputació de Catalunya (CESCA). We also thank Professor M. Bénard for further discussions and for reading the manuscript.

Supporting Information Available: A listing of HF Cartesian coordinates for anions **1** to **4** (7 pages). Ordering information is given on any current masthead page.

IC960222R

(30) Bader, R. F. W.; Henneker, W. *J. Am. Chem. Soc.* **1965**, *87*, 3063.
(31) Bader, R. F. W.; Preston, H. J. T. *Int. J. Quantum Chem.* **1969**, *3*, 327.
(32) MacDougall, P. J.; Schrobilgen, G. J.; Bader, R. F. W. *Inorg. Chem.* **1989**, *28*, 763.
(33) In Bader's formalism, an atom is a region of real space that contains a single nuclear attractor and is bounded by a zero-flux surface. The critical points in the charge density distribution, points where $\nabla\rho = 0$, play a prominent role in the boundary definition of an atom. In the interatomic surface of a diatomic molecule, all the gradient paths originate at the bond critical point which links the atoms of the molecule. In polyoxoanions, an example of this kind of elementary interatomic surface is found in the terminal oxygen atoms, which are bonded to only one metal center. The other atoms, however, exhibit very complicated interatomic surfaces. For example, the zero-flux surface which defines the volume of the central oxygen atom in the M_6O_{19} framework contains 30 critical points (7 bond critical points, 15 ring critical points, and 8 cage points). In contrast to a previous study[15] on $V_{10}O_{28}^{6-}$, in which the zero-flux surface for several atoms could not be established, the charge density integration was carried out for all $Nb_2W_4O_{19}^{4-}$ atoms. This was viable since an optimal geometry was used in the topological analysis of charge density.